# Remote Health Monitoring for Offshore Machines, using Fully Automated Vibration Monitoring and Diagnostics

**Mustapha Mjit, Pierre-Philippe J. Beaujean, and David Vendittis**

*Florida Atlantic University, SeaTech, 101 North Beach Road, Dania Beach, FL 33004 USA*
*mmjit@fau.edu*
*pbeaujea@fau.edu*
*DVendittis@aol.com*

**ABSTRACT**

This paper describes the use of vibration analysis with a fully automated diagnostics system to detect common machine faults such as imbalance and misalignment as well as bearing and gearbox faults of offshore machines. Other faults types, e.g. when a large object hits the propeller blades may be detected using the STFT. As the mechanical properties of the structure can change because of changes of temperature and oil quality, these (and other) state data are also stored. The data fusion process is currently under work. Experiments were performed on a home cooling fan system to demonstrate and illustrate the faults detection capability of the vibration and diagnostics system. Vibration data were also acquired from selected equipment on a small boat with different combinations (on/off status) of the engine, generator and hydraulic pump. The trending and alarm features were demonstrated for the different types of data. The vibration and diagnostics system is implemented with threshold limits for the alerts and alarms corresponding to each technique. The model also allows for automatic storing of raw data periodically and after any deviations from normal conditions; i.e., when alerts are on.[1]

## 1. INTRODUCTION

Offshore machines are subject to high and varying loads and extreme environment conditions; therefore, they require real time and remote monitoring strategies (Sloan et al., 2009; Beaujean et al., 2009) especially since access to these offshore machines is difficult and costly. These strategies allow for early remedial actions to reduce both maintenance costs and/or premature breakdown. The first such machine being considered is an ocean (current) turbine; a generic depiction of the turbine is shown in Figure 1 (Driscoll et al., 2008 (1); Driscoll et al., 2008 (2)). This turbine will be outfitted in the near future with vibration monitoring sensors as well as state (e.g., temperature) and safety sensors.

This paper discusses several traditional and more advanced approaches, procedures and techniques to evaluate the health of machines, using vibration data. Such methods have been shown to be efficient for evaluating equipment/component health (e.g. motors, engines, pumps, compressors and generators), provided the data are properly acquired and alarm thresholds properly set. A LabVIEW model for vibration condition monitoring that contains several advanced diagnostic techniques was developed and demonstrated.

Note that the current status of the ocean turbine did not permit side-by-side comparison of in-laboratory and ocean measurements at the time of this publication. Such comparison is of the upmost importance and will be the topic of a future publication. Also, the objective of this paper is not a broad discussion on reliability issues of ocean turbines. For reference, a reliability assessment for ocean turbines was the topic of a previous publication (Sloan, Khoshgoftaar, Beaujean and Driscoll, 2009).

In addition, ANSYS modeling was used to estimate the dynamic response of the machine in it normal operating conditions and to determine the resonance

frequencies of its sub-components (Mjit, 2009). Finally, a LabVIEW program that may be used to perform resonance testing on the structures was also developed (Mjit, 2009).

One of the features of the analysis and diagnostics tool is the power spectral density (PSD) that is used for in-depth analysis of the vibration signal. The data are assumed stationary; however, the vibration data collected from the machine structure may be somewhat non-stationary in nature. Therefore, the PSD may not provide sufficient information about the presence of abrupt changes due to transients. If the kurtosis indicates the existence of transients, a Short Time Fourier Transform (STFT) - waterfall and/or spectrogram - is used to better describe how the transients affect the data.

If the machine speed is not constant, the bandwidth of the PSD and the cepstrum over which to perform trending can be specified in the LabVIEW model. Two different data trending techniques are implemented: basic trending with respect to the baselines and automatic trending of data relative to the previous ones (e.g., the average of the last 10 measurements). The later trending technique is more commonly used with new machines that do not have repeatable baselines, or after a major repair/overhaul.

The relationship between the impulse response of individual structural elements and the PSD of the vibration signal is not always obvious. Thus, the cepstrum is used to demodulate the vibration signal and allow for trending the quefrency peaks that correspond to the components of interest. The ocean turbine contains a tachometer that may be used to measure the rpm variation induced by current variation. These variations might need to be accounted for in the data processing by ordering the data; the power spectral density frequencies are normalized with respect to the rpm.

The vibration monitoring system has been developed by following the recommendations of the International Standards Organization (ISO) standards (ISO, 2002; ISO, 2005). These standards address the whole vibration monitoring process from sensor selection and data processing to diagnostics and maintenance recommendations. To increase the reliability of the fault identification and state prognostics resulting from monitoring the health of offshore machinery, fusion between vibration data, temperature, pressure, oil quality and electric parameters (Cook, 2010) is under work (Duhaney et al., 2010) and follows ISO standards (ISO, 2003 (1); ISO, 2003 (2); ISO, 2004). Since early detection is more critical for these machines, features such as kurtosis trending/mapping and cepstrum analysis have been included as primary tools. For example, data from the oil quality sensor and the temperature sensor near the gearbox might be consistent in indicating that a problem/fault is developing, especially if the kurtosis has increased.

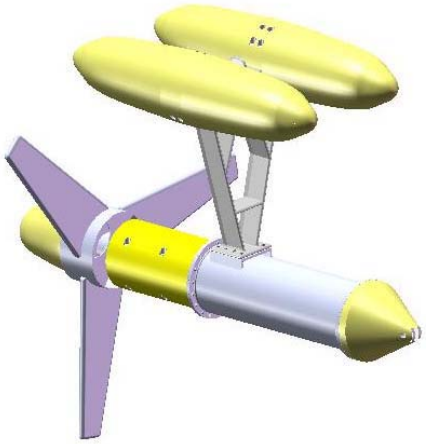

Figure 1: Ocean Turbine, Conceptual View (Driscoll et al., 2008 (2))

To gain experience in the acquisition, processing and interpretation of data similar to those expected from the ocean turbine, a dynamometer (Figure 2) that replicates the actual dynamics of the ocean turbine prototype was built. With the exception of fluid loading, the data acquired are similar to those expected from the actual turbine. Therefore, the monitoring algorithm developed here can be evaluated with inputs that are similar to those expected from the turbine sensors. The dynamometer will be operated at several rpm (steady state and intermittently). Data will be acquired to determine the process stationarity and the signal-to-noise ratio at selected frequencies (e.g., bearing frequencies).

The dynamometer contains a low speed motor, along with its shaft and bearings, connected to a gearbox (the gear box ratio is 25:1). The high speed shaft is connected to the electric motor/generator used in the ocean turbine. Since the dynamometer was not operational at the time of this publication, some experiments were performed on a fan to demonstrate and illustrate the faults detection capability. Vibration tests were performed at different speeds of the fan to relate the peaks in the PSD to the rpm and its harmonics. A second phase of the experiments utilized the fan running normally with no faults and the fan running when an object

was added to one of its blades to simulate an imbalance. Vibration data were also acquired from selected equipment on a small boat with different combinations (on/off status) of the engine, generator and hydraulic pump.

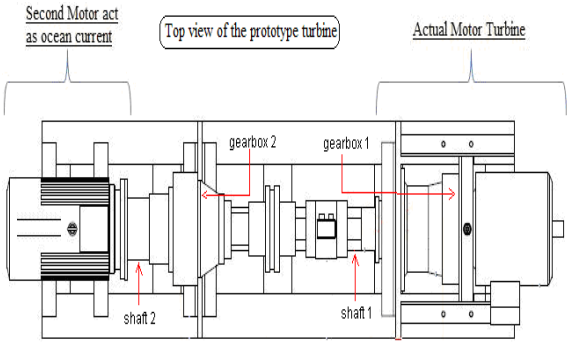


Figure 2: Dynamometer, Conceptual View

## 2. TECHNICAL DISCUSSION

Vibration condition monitoring is accomplished using fault detection and diagnostics. Fault detection is mainly concerned with detecting abnormal conditions in running machines. Fault diagnostics is the process of analyzing the data in order to accurately determine the type of fault, its severity and its location. Faults may be detected, and identified, by trending over equal intervals of time variations. A baseline spectrum is derived by either measuring the vibration levels on a machine in its normal operating conditions or derived statistically from a population of similar machines. A subset of the common techniques used for fault detection and diagnostics using vibrations data are shown in Table 1. They are described in (ISO, 2002; ISO, 2005), and discussed in (Beaujean et al., 2009; Mjit et al., 2010) relative to implementation for monitoring offshore machines.

It should noted that some faults do not necessarily result in an increase of the overall level thresholds; a strong vibration component from another source can mask a change and the machine could very well fail long before the fault can be detected. Therefore, it is highly desirable to compare and trend the vibration data to a baseline spectrum only when an adequate signal-to-noise ratio exists. De-noising techniques are being studied as a way of potentially mitigating the problem (Duhaney et al., 2010).

### 2.1 Kurtosis

The kurtosis is a statistical parameter, derived from the fourth statistical moment about the mean of the probability distribution function of the vibration signal and is an indicator of the randomness of that function. The kurtosis approach has the major advantage that the calculated value is independent of load or speed variations. The kurtosis value is a good parameter for fault and transient detection, but it does not always give an indication of the cause of the problem. The kurtosis will be equal to 3 for healthy machine and greater than 3 if the machine develops some faults that generate transients.

### 2.2 Frequency Domain Vibration Analysis

Typical frequencies associated with common faults are shown in Table 1. Frequency–based analysis techniques are quite useful for analyzing and trending stationary signals whose frequency components do not change over time.

Table 1: Common faults and corresponding frequencies

| Forcing Frequency | Fault |
|---|---|
| 1 x RPM | Imbalance-Misalignment-Bent shaft |
| 2 x RPM | Misalignment-Bent shaft |
| Harmonics of RPM | Loose bearing caps |
| Non-integer multiples of RPM | Rolling bearings-Gears |
| Number of teeth time RPM and harmonics | Gear faults |

1. PSD and Constant Percentage Band (CPB) analysis: The PSD is derived from the vibration waveform by performing a Fast Fourier Transform (FFT) or a CPB filtering operation. Because the speed of the shaft can slightly change over time, and to have accurate results, the LabVIEW program can normalize the power spectrum iteratively. The normalized fundamental frequency (measured by the encoder) is equal to 1. The normalized peaks in the spectrum are related to machine components (e.g., the level of a peak at a frequency corresponding to the shaft's rotation). In order to have accurate results, the sampled time period should be set so that it is a little longer than the period of revolution of the shaft.

2. Spectral data trending and baseline comparison: Trending the current spectrum and comparing it with the baseline spectrum was found to be a good indicator of many problems, including unbalance, misalignment, and bearing damage. The use of logarithmic scaling for the amplitudes was found to be very useful. The use of fractional (third octave or greater) octave data has proven to be more efficient way of trending the data. Once an alert/alarm is present, a more refined spectral analysis may be used.

### 2.3 Quefrency Vibration Analysis

The real cepstrum is the spectrum of the logarithm of the spectrum; it is used to highlight periodicities in the vibrations spectrum, in the same way the spectrum is used to highlight periodicities in the time waveform. Thus, harmonics and sidebands in the spectrum are summed into one peak in the cepstrum (called rahmonic), allowing simplified identification and trending of specific fault frequencies. It has been found to be useful in bearing and gearbox analysis.

The cepstrum is a very good indicator for bearing and gearbox faults. It is used for both faults detection and diagnostics. For fault detection, the data of harmonics and sidebands are reduced to one line and is not subjected to amplitude and frequency modulation for fault diagnostic. The application to operational modal analysis is based on the fact that the cepstrum of a response signal can be divided into its components from the forcing function and transfer function, thus allowing determination of the structural dynamic properties from response measurements alone. The trending of the cepstrum is primarily used to detect low frequency bearing faults that cannot be easily detectable by trending the PSD.

### 2.4 Time-Frequency Vibration Analysis

When the rpm of the shaft is changing over time due to short transient effects or due to variances in load, or when the shaft begins to develop a fault, the frequency changes over time cannot be easily observed on a time-averaged PSD. In some cases, two different signals, one stationary and the other with short transient effects can have the same spectrum, as shown in Figure 3. The presence of transient is indicated by a high crest factor and/or a high kurtosis value. In this case, a Time Frequency (TF) analysis is used, traditionally implemented with an STFT algorithm (Mjit et al., 2010),

$$PS(t,f) = \left|STFT(t,f)\right|^2 = \left|\int_{-\infty}^{+\infty} s(t')w(t'-t)e^{-j2\pi ft'}dt'\right|. \quad (1)$$

$PS(t,f)$ is power spectrogram of the signal $s(t)$ and $w(t)$ is a real and symmetric window translated by $t$.

TF analysis results are displayed in a spectrogram, which displays the vibration energy distribution in the time-frequency domain. In Figure 3, the two signals are similar, with signal 2 containing transient effect. The power spectra of both signals are almost identical because the energy of this transient spike is low and spread over a wide range of frequencies but the two signals do not have the same spectrogram.

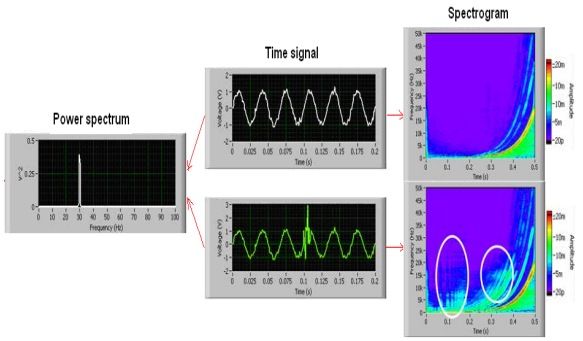


Figure 3: Time-Frequency Analysis

## 3. HARDWARE AND SOFTWARE ANALYSIS TOOL

The software developed is designed to collect, analyze, record, and post process recorded data, using the IO-Tech WaveBook/516E, WBK18 and WBK17 acquisition systems and accelerometers. It can collect, display and analyze multiple channels of data in real-time. The graphical displays consist on the time-domain data, frequency domain data, time-frequency domain data and quefrency data (Beaujean et al., 2009; ISO, 2003 (1)).

The software also performs the computation of the overall vibration level (RMS, peak, crest factor, kurtosis). The bandwidth of the PSD and cepstrum can be changed based on operating conditions (varying rpm). To minimize false alarms, trending is performed over narrow frequency bands at low frequencies, and over wide frequency bands at high frequencies. If the rpm changes exceed 10%, ordering may be needed. The software can perform the ordering operation of the PSD, third-octave spectrum and spectrogram with respect to the shaft speed (data from the tachometer).

This software is implemented with alerts and alarms criteria for all the diagnostics techniques features mentioned above. If the vibration levels exceed their respective baselines, an alert is activated and stays on until the vibration levels decrease sufficiently. This software can record the raw time signal on every channel, so that post processing with a different technique is possible. For example, a raw signal may be played back using different FFT Window algorithms to increase resolution. Once the desired results have been achieved, the new data may be exported to a different file and format, while preserving the original file.

For long term monitoring, the model allows for the automatic storing of raw data periodically and after any deviations from normal conditions, i.e., when alerts are on. This makes it possible to follow the progress of the faults without saving data continuously.

## 4. EXPERIMENTAL RESULTS

To illustrate the features of the monitoring system, some experiments were performed on a commercial fan and on a small boat in different situations. For the experiments on the fan, the featured techniques were:

1. The determination of the minimum number of average, needed for this system running at 450 rpm.
2. The correlation of the peaks, in the PSD and in the cepstrum, to the forcing frequencies for the healthy system running at 450 rpm and 840 rpm.
3. The illustration of the effect of the imbalance fault on the PSD and on the cepstrum, and comparison with the theory.
4. Order "Normalization" analysis of the PSD for the system running at 450rpm.
5. The illustration of the effect of transient effect on the kurtosis and on the STFT by hitting the fan while running and using a hammer with a calibrated force transducer.

The fan has five blades and the sampling frequency was set to 1000Hz in order to pick two families of harmonics (1 time the rpm and 5 times the rpm, related to the five blades). Cepstrum analysis was used to collapse the two families of harmonics into two peaks. 3000 scans were acquired each iteration giving a frequency resolution of 0.33 Hz.

The data were acquired from a low frequency accelerometer mounted on the fan casing using adhesive. The AC136-1A, low noise accelerometer had the following specifications: sensitivity of 500 mV/g, pass band frequency response between 0.2 and 3000 Hz, and very low noise PSD of 1.7 μg/√Hz at 10 Hz. An 8-pole Butterworth analog low-pass filter was used to achieve a good attenuation in the stop band and minimal distortion in the pass-band. Its cut-off frequency was set to 200 Hz to avoid aliasing.

The power spectral density, displayed in decibel (dB) was computed using a Hanning window (to minimize the frequency distortion due to block averaging), in both RMS averaging mode and linear time averaging.

For the experiment on a small boat, the features techniques demonstrated were:

1. The correlation of the spikes in the PSD to the cylinders firing rate using three different speed of the engine 700, 1400 and 2100 rpm.
2. The illustration of the effect of each component separately on the PSD by running the experiment with different combination (on/off status) of the main engine, hydraulic pump and generator.
3. The comparison of the acquired data to their baseline in two different situations (Figures 18 and 19).

The accelerometers (AC136-1A) were mounted on the gearbox (HF), main engine (LF), generator (HF) and pump (LF), respectively. The sampling frequency was 8000Hz, and 8000 scans-per-second were acquired, leading to a frequency resolution of 1Hz. An 8-pole low pass filter was used with a cut-off frequency was set to 2 kHz. In the following results, a data sample is defined as a 10 second average (80,000 scans).

### 4.1 Fan results

The minimum number of PSD averages for the fan is determined using the following rule: record two spectra, the first one with N averages and the second with 2xN averages. If the spectra are significantly different, the number of averages should be doubled again and another spectrum recorded. If the latter two spectra are similar, then the previous number of averages is adequate for the vibration PSD analysis.

In Figure 4, two vibration signals are compared. The green signal is the result of averaging 10 samples and the red signal is from one sample. We notice a difference between the signals due to the noise errors. This noise will cancel out by the averaging process, thus, the importance of averaging the signal.

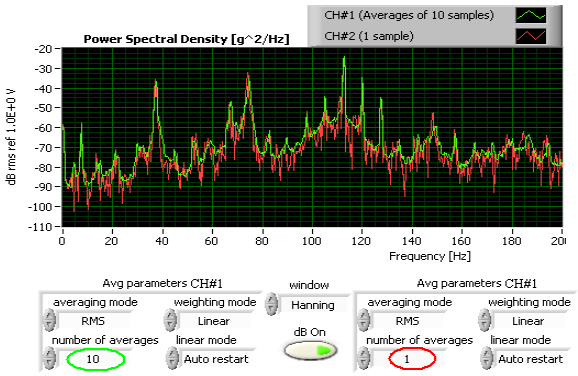


Figure 4: Spectral averaging of the fan vibration measurements (1 or 10 averages) at 450 rpm

In Figure 5, the acceleration signal with two different averaging numbers (green one with 10 averages, and the red one with 20 averages) are compared. The two acceleration signals are almost identical, thus 10 averages are adequate to study the vibrations of this fan.

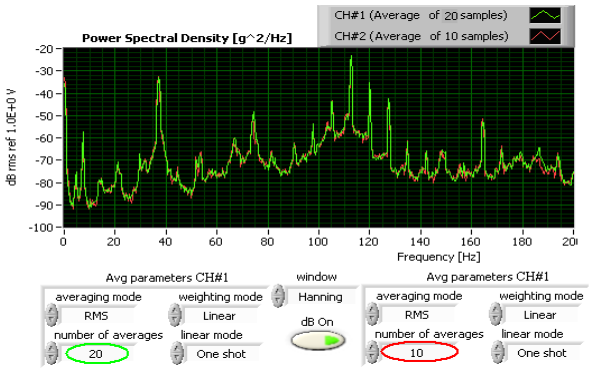


Figure 5: Spectral averaging of the fan vibrations (10 or 20 averages)

In Figure 6, the PSD displays harmonics of 14 Hz (840 rpm). In particular, the fundamental (14 Hz) and fifth harmonic (70 Hz, or the number of blades times the fundamental) are very strong. The bearings tones are also observed at 4.2 Hz and 7 Hz (0.3 and 0.5 times the fundamental).

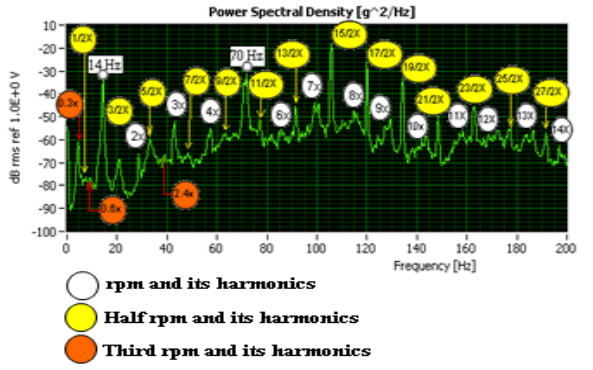


Figure 6: PSD of healthy fan running at 840 rpm

The cepstrum analysis is used to quantify periodical information of spectral data. As shown in Figure 7, the cepstrum summarizes all families of harmonics in the PSD within single values, e.g. the families of the peaks correspond to the rpm (1X, 5X) and their harmonics, bearings tones (0.3X, 0.5X) and theirs sidebands, are reduced to singles peaks in the cepstrum. Still in Figure 7, the table below the graph displays automatically the four largest peaks quefrencies and frequencies and the bearings tones appear separately from the blades tones.

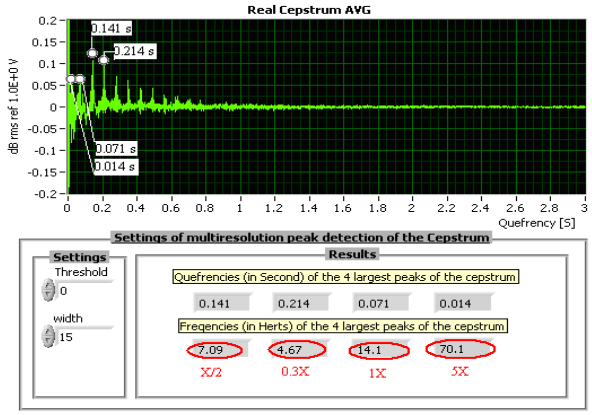


Figure 7: Harmonic separation using the cepstrum analysis tool, for healthy fan running at 840 rpm

In Figure 8, the fan was running at low speed (450 rpm) which resulted in bearing tones of lesser amplitude. In addition, bearings sidebands do not appear in the PSD plot. As in the previous case, all the families of harmonics in the PSD (0.5X, X, 5X) are reduced to single peaks in the cepstrum (Figure 9). The imbalance fault was introduced by attaching a small load to one of the fan blades. Figure 10 illustrates the effect of the imbalance on the PSD. As expected from the theory, the imbalance generates strong vibration amplitudes at the fundamental frequency (1X) and its first and second harmonics (2X, 3X), but only some vibration at higher harmonics orders.

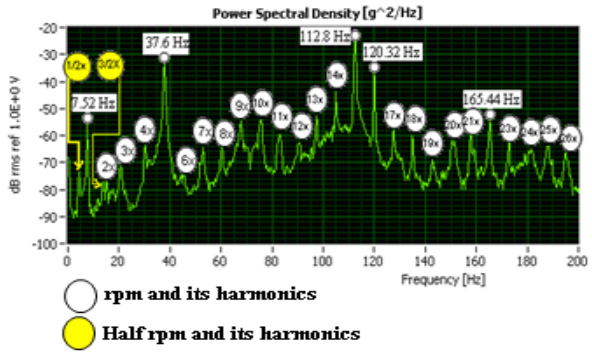


Figure 8: PSD of healthy fan running at 450 rpm

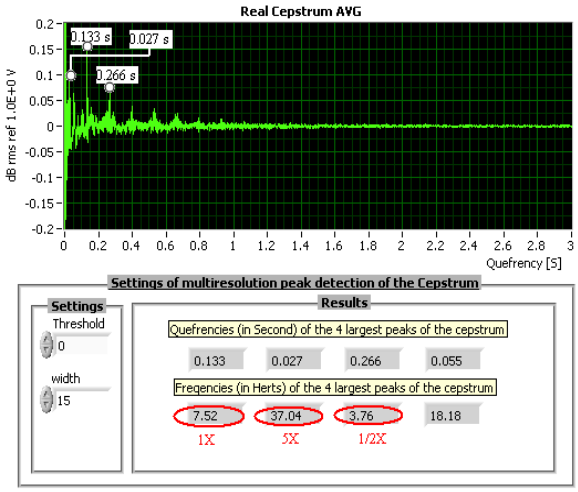


Figure 9: Harmonic separation using the cepstrum analysis tool, for healthy fan running at 450 rpm

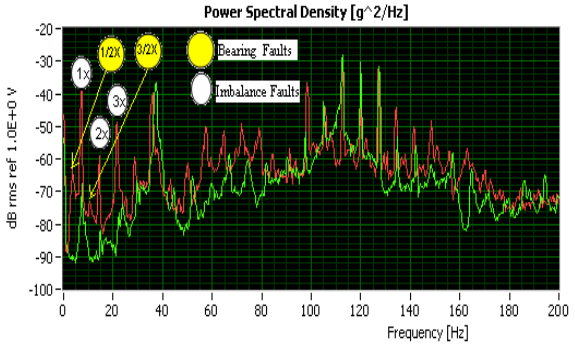


Figure 10: PSD of healthy Fan (green curve) and with imbalance fault introduced (red curve) (450 rpm)

In Figure 11, The PSD is normalized with respect to the rpm, and the data are displayed in term of multiples and fractional of the rotational speed. The fundamental of the rpm and its harmonics are integers, and bearings tones are not integers. The advantage of this ordering technique is the ability to clearly identify the peaks related to the forcing frequencies and those that are caused by the inception of anomalies in the system. Another important advantage of the ordering process is that the spectra have peaks at the same orders during measurements and can easily be averaged without smearing.

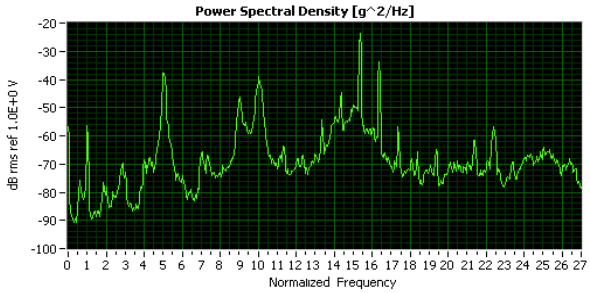


Figure 11: Normalized PSD with respect to the rpm (450 rpm)

In Figure 12, the kurtosis, STFT waterfall and spectrogram are acquired from the fan running at 840 rpm. The kurtosis is constant with respect to time and does not exceed the thresholds limits. Thus the alert and alarm are "off". In Figure 13, the kurtosis, the STFT waterfall and the spectrogram are acquired from the fan running at 840 rpm while a transient effect is produced by hitting the fan casing with a hammer. The kurtosis increases, exceeds the threshold limits and triggers an alert. For more details on how this transient effect affects the data, the waterfall and the spectrogram can be used. Both plots show a high level of -30dB after 2.3 second in following frequency bands: 180-200 Hz, 90-150 Hz and 65-70 Hz.

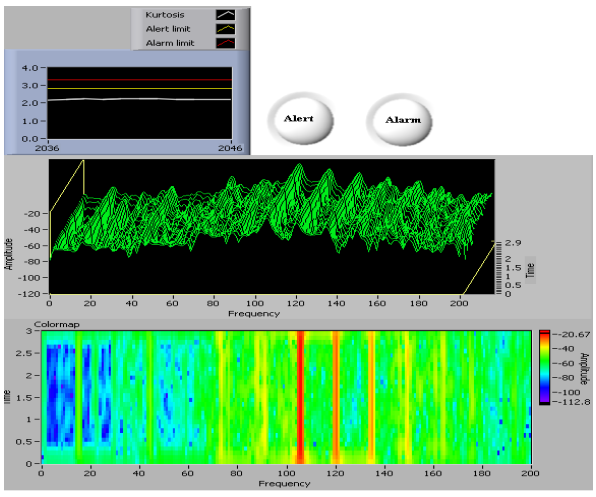


Figure 12: Kurtosis, STFT waterfall and kurtosis and its alert and alarm features for the fan running at 840 rpm

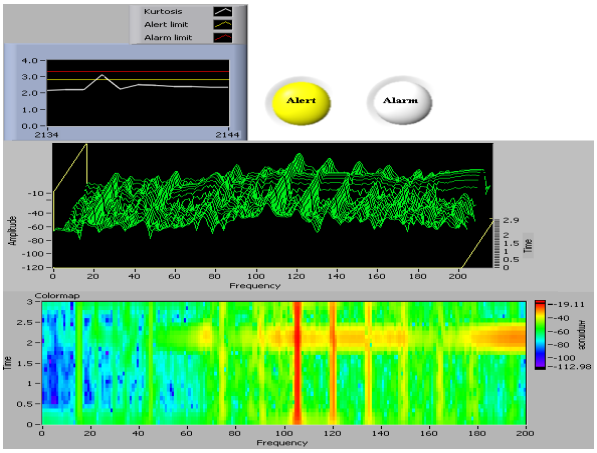


Figure 13: Waterfall, Spectrogram, kurtosis and its alert and alarm features for the fan running at 840 rpm while a small transient effect was introduced

In a second test, the kurtosis, STFT waterfall and spectrogram are acquired under the same conditions except for a stronger hammer impact, The kurtosis increases and exceeded both alert and alarm thresholds limits, Figure 14. This time (after 1.5 second), the transient effect affect the following frequency bands: 120-200 Hz and 90-96 Hz.

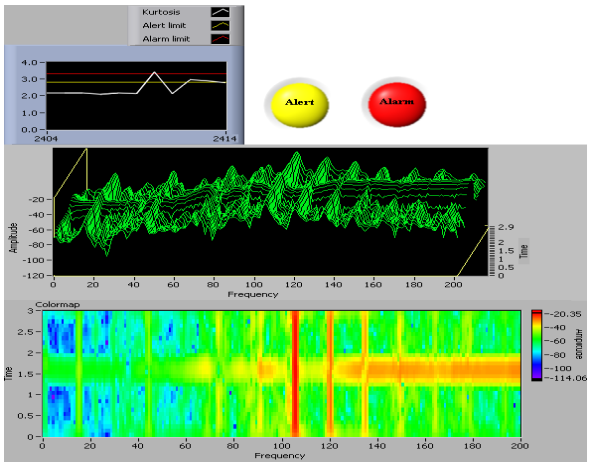


Figure 14: Kurtosis, STFT waterfall, spectrogram, alert and alarm features for the fan running at 840 rpm while a large transient effect is produced

### 4.2 Boat results

With the small boat experiment, we demonstrate the correlation of the PSD spikes to the cylinders firing rate using three different speed of the engine: 700, 1400 and 2100 rpm. We then illustrate the effect of each component on the PSD separately by running the experiment with different combination (on/off status) of the main engine, hydraulic pump and generator. A high frequency accelerometer was mounted on the gearbox. Figure 15 shows the PSD of the data acquired at three different speed of the main engine: 700, 1400 and 2100 rpm. The harmonics corresponding to the cylinder firing rate for each speed (5.8, 11.6 and 17.5 Hz) clearly appear.

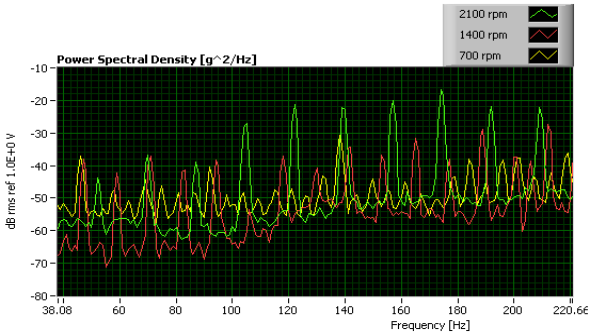


Figure 15: PSD of the data acquired at three different speeds 700, 1400 and 2100 rpm (one sample)

To illustrate the effect of the generator on the PSD, two different vibration tests were performed; the green and red curves in Figure 16 correspond to the PSD of data acquired when the main engine alone is on, and when both the main engine and the generator are on respectively. As expected, the generator introduces some noise and more peaks on the PSD.

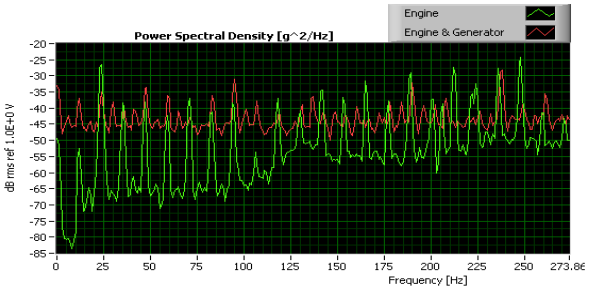


Figure 16: PSD of the data acquired in two different situation: engine on, both engine & generator on (one sample)

To show the effect of both the generator and the hydraulic pump on the PSD, the experiments were performed when the main engine alone is on (green curve), and when the main engine, generator and hydraulic pump are on (red curve), Figure 17. The generator and the hydraulic pump generate more peaks in the PSD.

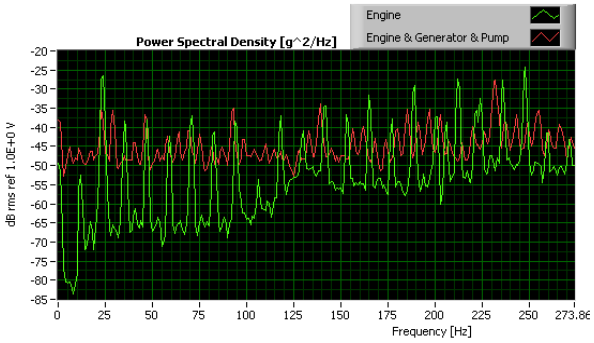


Figure 17: PSD of the data acquired in two different situations: engine on, and engine, generator and pump on (one sample)

This experiment also includes the comparison of the acquired data to their baseline in two different situations (Figures 18 and 19). In Figure 18, the current third octave is compared to the previous one for the engine running at 2100 rpm. Nothing changes and alert and alarm are off. In Figure 19, the third octave of the vibration data acquired at 2100 rpm is compared to the third octave of the data acquired at 1400 rpm (baselines). The discrepancy in multiple third-octave bands results both in an alert and alarm.

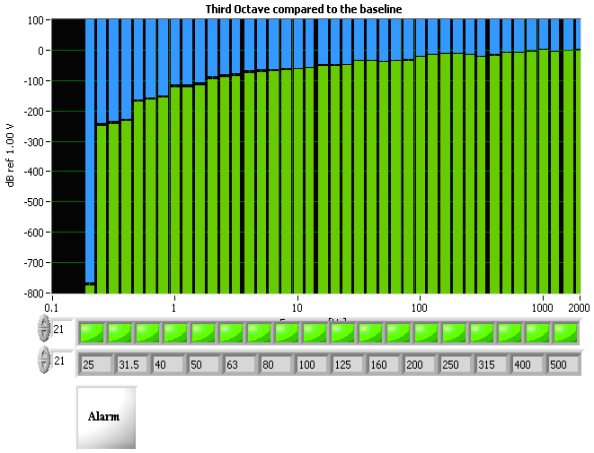


Figure 18: Combined vibration data processing, alerts and alarms, 2100 rpm (one sample)

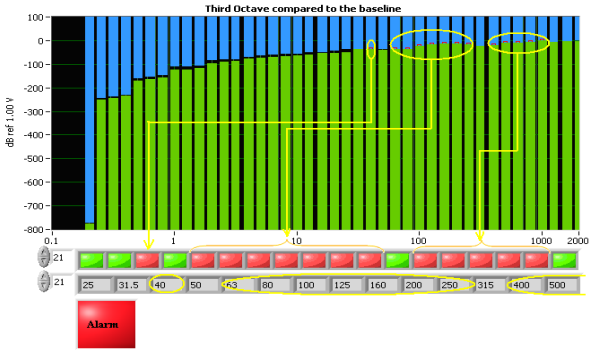


Figure 19: Combined vibration data processing, alerts and alarms, regime change from 2100 rpm to 1400 rpm (one sample)

Each third-octave band producing an alert or alarm can be closely analyzed using the PSD output. As an example, in Figure 19, the third-octave bands at center frequencies 40, 125, and 250 Hz produce alerts. As shown in Figure 20, the spikes that cause the three third octave bands to exceed their respective baselines are: (1) 35.7 Hz for the first band; (2) 122Hz and 139.2Hz for the second band; (3) 227.1Hz, 243.8Hz, 262Hz and 278.6Hz for the third band. These frequencies correspond to harmonics of the cylinder firing rate (17.5 Hz).

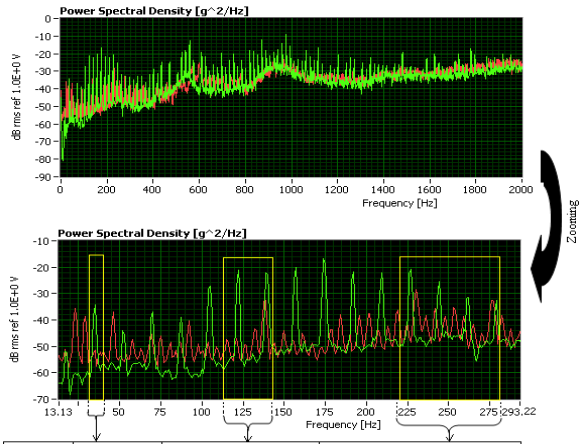


| 1/3 Octave Band Center Freqency | 40 Hz | 125 Hz | 250 Hz |
|---|---|---|---|
| Bandwidth (Hz) | [35.6 - 44.9] | [111.4 - 140.3] | [222.7 - 280.6] |

Figure 20: PSD analysis (one sample), red curve represents the PSD baseline (2100 rpm) compared to the green curve (1400 rpm)

## 5. CONCLUSION

The vibration monitoring and diagnosis tool has been presented in this paper. This tool, designed to initially monitor an ocean turbine, has the following capabilities: (1) automatic storage of raw data periodically and after any deviation from normal conditions; (2) multiple trending techniques; (3) early failure identification of the faults through generation of alerts before dangerous vibration condition of the machine occurs; (4) ordering of the frequency data with respect to the shaft rpm; (5) reduction of maintenance cost by isolation, localization and diagnosis of vibration causes. At-sea demonstration of this tool will be performed on an ocean turbine prototype in the near future. In the meantime, it has been tested on a small boat and on a fan system and is now being installed on a dynamometer.

## REFERENCES


Beaujean, P. P., Khoshgoftaar, T. M., Sloan, J. C., Xiros, N., Vendittis, D. (2009). Monitoring Ocean Turbines: a Reliability Assessment, in *Proceedings of the 15th ISSAT International Conference on Reliability and Quality in Design*, San Francisco, California.

Cook, K. (2010), M.S. Thesis. *A Power Quality Monitoring System for the Center Of Ocean and Energy Technology's Ocean Turbine.* Florida Atlantic University.

Duhaney, J., Khoshgoftaar, T.M., Alhalabi, B. and Sloan, J. C. (2010). Applications of Data Fusion in Monitoring Inaccessible Ocean Machinery in *Proceeding of the 16th ISSAT International Reliability and Quality in Design conference*, 2010, Washington, D.C.

Driscoll, F. R., Skemp, S. H., Alsenas, G. M.C., Coley C. and Leland, A. (2008). Florida Center for Ocean Energy Technology in *Proceedings of the MTS/IEEE Oceans 2008*, Quebec City, Canada.

Driscoll, F. R., Alsenas, G. M., Beaujean, P. P., Ravenna, S., Raveling, J., Busold, E. and Slezycki, C. (2008). A 20 kW open ocean current test turbine in *Proceedings of the MTS/IEEE Oceans 2008*, Quebec City, Canada.

ISO (2002), Condition monitoring and diagnostics of machines - Vibration condition monitoring - Part 1: General procedures, in *ISO13373-1:2002*. Ed.:ISO.

ISO (2003), Condition monitoring and diagnostics of machines - General guidelines, in *ISO17359:2003*. Ed.: ISO.

ISO (2003), Condition monitoring and diagnostics of machines - General guidelines on data interpretation and diagnostics techniques, in *ISO13379:2003* . Ed.: ISO.

ISO (2004), Condition monitoring and diagnostics of machines – Prognostics-Part1: General guidelines, in *ISO13381-1:2004*. Ed.:ISO.

ISO (2005), Condition monitoring and diagnostics of machines - Vibration condition monitoring - Part 2: Processing, analysis and presentation of vibration data, in *ISO13373-2:2005*. Ed.:ISO.

Mjit, M. (2009), M.S. Thesis. *Methodology for fault detection and diagnostics in an ocean turbine using vibration analysis and modeling.* Florida Atlantic University.

Mjit, M., Beaujean, P.-P. J. and Vendittis, D.V (2010) Fault Detection and Diagnostics in an Ocean Turbine using Vibration Analysis in *Proceedings of ASME IMECE10*, Vancouver, Canada.

Sloan, J. C., Khoshgoftaar, T. M., Beaujean, P. P., Driscoll, F. (2009). Ocean Turbines – a Reliability Assessment, *International Journal of Reliability, Quality and Safety Engineering*, vol. 16, issue 5, pp.1-21.